

Laser desorption/ionization mass spectrometric study of secondary organic aerosol formed from the photooxidation of aromatics

Mingqiang Huang · Weijun Zhang · Liqing Hao ·
Zhenya Wang · Wenwu Zhao · Xuejun Gu ·
Xiaoyong Guo · Xianyun Liu · Bo Long · Li Fang

Received: 3 September 2007 / Accepted: 12 November 2007 / Published online: 13 December 2007
© Springer Science + Business Media B.V. 2007

Abstract Five aromatic hydrocarbons – benzene, toluene, ethylbenzene, *p*-xylene and 1,2,4-trimethylbenzene – were selected to investigate the laser desorption/ionization mass spectra of secondary organic aerosols (SOA) resulting from OH-initiated photooxidation of aromatic compounds. The experiments were conducted by irradiating aromatic hydrocarbon/CH₃ONO/NO_x mixtures in a home-made smog chamber. The aerosol time-of-flight mass spectrometer (AToFMS) was used to measure the aerodynamic size and chemical composition of individual secondary organic aerosol particles in real-time. Experimental results showed that aerosol created by aromatics photooxidation is predominantly in the form of fine particles, which have diameters less than 2.5 μm (i.e. PM_{2.5}), and different aromatic hydrocarbons SOA mass spectra have eight same positive laser desorption/ionization mass spectra peaks: *m/z*=18, 29, 43, 44, 46, 57, 67, 77. These mass spectra peaks may come from the fragment ions of the SOA products: oxo-carboxylic acids, aldehydes and ketones, nitrogenated organic compounds, furanoid and aromatic compounds. The possible reaction mechanisms leading to these products were also discussed.

Keywords Aromatic hydrocarbons · Secondary organic aerosols · Smog chamber · Laser desorption/ionization · Reaction mechanism

1 Introduction

Aromatic hydrocarbons are an important class of organic compounds in urban and regional atmosphere, and released into the atmosphere by human activities, such as emissions from burning oil and coal, motor vehicle exhaust, evaporation of solvents and emission from gasoline stations. Besides the toxicity to humans, conversion of aromatic hydrocarbons in the atmosphere can play a significant role in the increase of ozone concentration in

M. Huang · W. Zhang (✉) · L. Hao · Z. Wang · W. Zhao · X. Gu · X. Guo · X. Liu · B. Long · L. Fang
Laboratory of Environment Spectroscopy, Anhui Institute of Optics and Fine Mechanics, Chinese
Academy of Sciences, Hefei 230031, People's Republic of China
e-mail: wjzhang@aiofm.ac.cn

troposphere as well as in the formation of secondary organic aerosol (SOA) (Odum et al. 1997). Interest in SOA formation in the atmosphere has been renewed because of its possible impacts on visibility of air (Pilinis et al. 1995), formation of clouds, change of the climate (Annamarie et al. 1993), and human health (Schwartz et al. 1996) seriously. In the last 10 years, the studies on formation mechanism (Andino et al. 1996; Forstner et al. 1997; Jang et al. 2001; Suh et al. 2002; Suh et al. 2003;) and detection methods (Yu et al. 1997, Forstner et al. 1997; Smith et al. 1998; Jang et al. 2001; Edney et al. 2001; Kleindienst et al. 2004) of SOA are interesting particularly. Chemical composition of SOA particles was often studied by off-line techniques. The particles were usually collected using filters or impactor plate and samples were prepared by the way of chemical extracts. Molecular composition of SOA particles could be analyzed by Gas Chromatograph/mass spectrometer (GC-MS), or positive chemical ionization (CI) gas chromatography ion trap mass spectroscopy (GC-TIMS) (Forstner et al. 1997; Smith et al. 1998; Jang et al. 2001; Edney et al. 2001; Kleindienst et al. 2004). By the way, the Fourier transform infrared spectroscopy (FTIR) was used to obtain additional functional group information for SOA products (Jang et al. 2001). However, there are some disadvantages in GC/MS and CI-GC-TIMS systems, for example, possible secondary chemical reactions or loss of semivolatile compounds associated with traditional aerosol sampling onto a filter or impactor plate, or with multi-step chemical treatments. In addition, it is difficult to measure the size and chemical compositions of the individual SOA particles simultaneously and in real-time by using the off-line techniques.

From the mid 1990s, real-time aerosol mass spectrometry has been remarkably developed, offering new opportunities for on-line studying aerosol particulate matters (Suess and Prather 1999). Most of those instruments can size, count, and mass-analyze individual particles with high time-resolution (Prather et al. 1994). Among such instruments, NOAA's Particle Analysis by Laser Mass Spectrometer (PALMS), Aerosol Time-of-Flight Mass Spectrometer (ATOFMS), Rapid Single-Particle Mass Spectrometer II (RSMS-II), and Aerodyne's Aerosol Mass Spectrometer (AMS) were operated together during the Atlanta Supersite Project to characterize the performance of the instruments (Middlebrook et al. 2003). Although these mass spectrometers are generally classified as similar instruments, they clearly have different characteristics due to their unique designs. One primary difference is related to the volatilization/ionization method: PALMS, ATOFMS, and RSMS-II utilize laser desorption/ionization, whereas particles in the AMS instrument are volatilized by impaction onto a heated surface with the resulting components ionized by electron impact. Thus mass spectral data from the AMS are representative of the ensemble of particles sampled, and those from the laser-based instruments are representative of individual particles (Middlebrook et al. 2003). The application of these instruments to the SOA particles was started in the 2001. Angelino et al. (2001) used ATOFMS to characterize the aerosol particles formed from reactions of secondary and tertiary alkylamine. On-line measurement of SOA particles formed from photooxidation of 1,3,5-trimethylbenzene using ATOFMS and AMS was conducted by Gross et al. (2006) and Alfara et al. (2006) respectively. The AMS employs a 70 eV electron impact ionization (EI), which causes a significant fragmentation of the organic molecules. However, for the high laser intensity required to desorb and ionize the particle, organic ions generated will readily absorb multiple UV photons resulting in massive fragmentation. Silva and Prather (2002) have found that in many cases, positive ion mass spectra of organic compounds are similar to those found in libraries for 70-eV electron impact mass spectrometry. So, it is not a surprise that both Gross et al. (2006) and Alfara et al. (2006) obtained small fragment mass spectra peaks of the 1,3,5-trimethylbenzene SOA particles, including some of the same fragment mass spectra peaks, such as m/z 27, 43.

Alfarra et al. (2006) showed that the contributions of m/z 43, 44, 46 (may arise from CH_3CO^+ , CO_2^+ , NO_2^+) could serve as atmospheric tracers for the aerosols produced from the photooxidation of 1,3,5-trimethylbenzene which was oxidized in nature and dominated by carbonyl-containing, multifunction carboxylic acid and nitrogenated organic compounds. Indeed, Forstner et al. (1997) and Yu et al. (1997) found that many individual aromatic species generate similar (and in some cases identical) atmospheric oxidation products. So the secondary organic aerosol from different aromatic compounds may contain some same mass spectra peaks. To the best of our knowledge, no investigations on the mass spectra peaks of SOAs from different aromatic compound are performed up to now. Our laboratory has demonstrated that ATOFMS can be used to measure the size and chemical composition of toluene SOA particles in real-time (Wang et al. 2006). So, in this paper, the photooxidation of five aromatic hydrocarbons – benzene, toluene, ethylbenzene, *p*-xylene and 1,2,4-trimethylbenzene (1,2,4-TMB) was initiated by hydroxyl radical (OH) to form SOA in a home-made smog chamber, ATOFMS was employed to detect the individual particles in real-time. Our goal is to obtain the positive laser desorption/ionization mass spectra of SOA particles from photooxidation of different aromatic compounds. From the mass spectra of a large number of individual particles, we can get the main mass spectra peaks statistically.

2 Experimental methods

2.1 Aerosol time-of-flight mass spectrometer (ATOFMS)

Aerosol time-of-flight mass spectrometer includes three distinct regions: (1) an aerosol introduction interface, which includes three adjustable stages of differential pumping; (2) a light scattering region for particle detection and velocity/size determination; and (3) a linear-time-of-flight mass spectrometry for single particle composition analysis (Xia et al. 2006a, b). Figure 1 shows a simplified drawing, highlighting key instrumental features, and provides a reference for a general overview of instrument operation. Particles are introduced into the instrument through a converging nozzle. The nozzle is separated from a skimmer and the region is mechanically pumped to a pressure of ~ 2 Torr. The expansion of molecules in this region accelerates the particles to velocities dependent on their aerodynamic size. A secondary skimmer allows for differential pumping to reach the pressures needed to operate the mass spectrometer and collimates the particle beam by removing particles that do not follow a straight trajectory through the nozzle. Then the particle beam is transmitted into the light scattering region where they encounter two red continuous-wave, diode-pumped lasers at 650 nm (50 mW) separated by 70 mm through differentially pumped stages with two skimmers. The lasers are positioned perpendicular to one another and orthogonal to the particle beam. For each laser, an arrangement of optics is used to focus the laser beam to a spot that intersects the particle beam. A particle passing through each laser beam scatters light which is collected by an ellipsoidal mirror and focused onto a photomultiplier tube (PMT) detector. The PMTs send pulses to an electronic timing circuit that measures the time required for the particle to travel the known distance between the two scattering lasers. The distance and the particle time-of-flight are used to calculate the particle velocity. An external size calibration uses particles of known size to relate the velocity to an aerodynamic diameter. The particle size calibration of ATOFMS is determined by sampling Dioctyl phthalate (DOP) particles producing by TSI 3450 and 3940 system (TSI Model 3450 and 3940). The detection efficiency for particles smaller than the

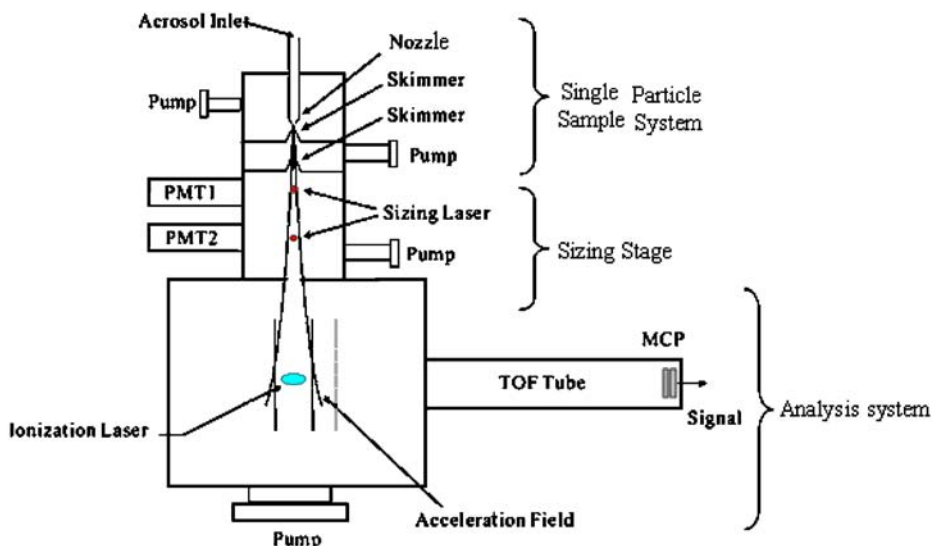


Fig. 1 Schematic of the Aerosol time-of-flight Mass Spectrometer

wavelength of the detection laser light is very low due to the Mie scattering process. Thus, the lower limit of the detected particles diameter is ~ 200 nm. Once the circuit begins a countdown to the time when the particle will reach the center of the ion source region of a mass spectrometer. At this time, the circuit sends a signal to a fire a pulsed excimer KrF laser at 248 nm having an average power density of $\sim 10^7$ W/cm² and a pulse length 2.5 ns. Upon absorption of the laser pulses, the particle is heated in a rapid fashion, desorbing and ionizing individual molecules from the particle. The resulting positive ions are mass analyzed in a linear time-of-flight mass spectrometer. Thus, for each particle analyzed, the size is obtained through the particle velocity and the corresponding particle composition is determined through the positive ion mass spectra.

2.2 Smog chamber experiment

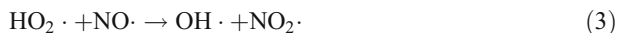
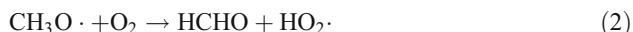
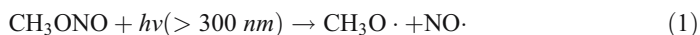
Benzene, toluene, ethylbenzene, *p*-xylene and 1,2,4-TMB (>99%) was obtained from Sigma-Aldrich Chemistry Corporation, Germany. Sodium nitrate (>99%) and methanol (>99%) were purchased from the Tianjin (The third Reagent Manufactory), and nitrogen oxide (99.9%) from Nanjing Special Gas Factory, which were used without further purification.

Methyl nitrite was synthesized by the dropping sulfuric acid into a methanol solution of sodium nitrate. Their reaction products passed through saturated sodium hydroxide trap to remove the traces of sulfuric acid, and were dried by passing through a calcium sulfate trap and collected using a condenser of liquid nitrogen at 77 K. The methyl nitrite was purified using a vacuum system of glass.

Photooxidation of aromatic hydrocarbon was performed using UV-irradiation of aromatic hydrocarbon/CH₃ONO/NO/air mixtures in an indoor evacuable photochemical smog chamber, the overall system components have been presented in detail previously (Hao et al. 2005) and will only be briefly described here. The experimental setup consists of a smog chamber and manifold system. The smog chamber is made of quartz tube, and its volume and the ratio of surface to volume are 23.3 liters and 22.4 m⁻¹ respectively. The reactor is surrounded by 16 fluorescent black lamps used to initiate the reactions. The output

power of each black lamp is 20 W and its wavelength of UV radiation is 300–400 nm. The volume of glass manifold system is 0.84 liter, equipped with a vacuum gauge whose measuring range is 10–5,000 Pa. Wall losses, probably significant in such a small chamber, were not a concern here given the aim of this study.

Prior to start each experiment, the chamber was continuously flushed with purified laboratory compressed air for 20 min, and evaluated to a vacuum of 10^{-1} Pa by a mechanical pump. The compressed air was processed through three consecutive packed-bed scrubbers containing, in order, activated charcoal, silica gel and a Balston DFU® filter (Grade BX) respectively, to remove the trace of hydrocarbon compounds, moisture and particles. Aromatic hydrocarbon was sampled by a micro liter injector and injected directly into the chamber. NO and methyl nitrate were expanded into the evacuated manifold to the desired pressure through Teflon lines, and introduced into the smog chamber by a stream of purified air. The whole system was completely shrouded from light with a black polyethylene tarpaulin. Hydroxyl radicals were generated by the photolysis of methyl nitrite in air at wavelengths longer than 300 nm (Atkinson et al. 1981). The chemical reactions leading to the formation of the OH radical are:



A series of experiments were carried out to investigate SOA from the OH-initiated oxidation of aromatic under the conditions summarized in Table 1. And the SOA particles produced by the photooxidation were analyzed by the ATOFMS connected directly to the chamber using a Teflon line.

3 Results

According to the design principles on the measuring system of particle diameter, timing circuit, and laser desorption/ionization (LDI) setup of ATOFMS, its time-of-flight mass spectroscopy is only obtained from those particles of secondary organic aerosol, whose

Table 1 Summary of the experimental conditions

Experiment no.	Aromatic ($\mu\text{L/L}$)	[Aromatic] ($\mu\text{L/L}$)	[CH_3ONO] ($\mu\text{L/L}$)	[NO]	4 black lamps
1	toluene	0	0	0	On for 2 h
2	toluene	200	0	0	On for 2 h
3	toluene	0	0	200	On for 2 h
4	toluene	0	1,000	0	On for 2 h
5	toluene	200	1,000	200	Off for 2 h
6	toluene	200	1,000	200	On for 2 h
7	ethylbenzene	200	1,000	200	On for 2 h
8	<i>p</i> -xylene	200	1,000	200	On for 2 h
9	1,2,4-TMB	200	1,000	200	On for 2 h
10	benzene	200	1,000	200	On for 2 h

diameter has been measured. The diameter of individual particle, number distribution of SOA particle diameter, and molecular composition of SOA particle could be measured using our ATOFMS.

3.1 Size distribution of aromatics SOA particles

The ATOFMS instrument, sampling through the nozzle inlet used here, is known to have size-dependent transmission of particles into the instrument. The transmission and detection for smaller particles is significantly less efficient than that for larger particles. And as described in the [Experimental methods](#) section, an external timing circuit sends a triggering pulse to fire the KrF laser when the sized particle arrives in the ion source region of the ATOFMS. In general, not all particles that are sized produce mass spectra. In this work, detection efficiency of the particles, D_E , is defined as the ratio between the number of particles hit by the LDI laser that generate ions detectable by the mass spectrometer and the number of particles sampled by the ATOFMS during the same time period, as described in the following equation:

$$D_E = N_H / C_{APS} Q$$

where N_H is the number of particles hit per minute (particles/min); C_{APS} is the particle number concentration measured by the TSI APS 3321 (TSI Model 3321) (particles/cm³), and Q is the flow rate of the sampling inlet (cm³/min). Particle detection efficiency is an important parameter for evaluating the performance of the ATOFMS, this parameter depends on the performance of the sampling inlet and the components used for light-scattering measurement, as well as on the particle size, shape, and chemical composition.

For experiment 1–5, nearly no particles were detected by the ATOFMS, indicating that aerosol particles arisen from the OH-initiated photooxidation of aromatics. Figure 2 shows the size distribution of the sized and hit particles as well as the variation of particle detection efficiency during aromatics photooxidation experiments. The current ATOFMS has detection efficiencies ranging as a function of particle size from ~25 to ~1% for aromatic SOA particles. As shown in Fig. 2, the detection efficiencies is relatively uniform for aromatic SOA particles between 600 and 1,200 nm but decreased nearly to zero below and above these values. And aerosol created by these aromatics are predominant in the form of fine particles, which have diameter less than 2.5 μm (i. e. PM_{2.5}), most of the SOA particles are about 600–1,200 nm. Researches have shown that these fine particulate matters are more easily deposit in the lung of the human being, and do great harmful to the health (Schwartz et al. 1996).

3.2 Laser desorption/ionization (LDI) mass spectra of aromatics SOA particles

In order to compare the mass spectra of different aromatic SOA particles, we selected two single particles for each aromatic hydrocarbon. The aerodynamic diameter and the corresponding positive laser desorption/ionization mass spectra of these individual aromatics SOA particles are shown in Fig. 3. It is told that each piece of mass spectrum corresponds to an aerosol particle, and the diameter and chemical composition might be different from each other. It indicated that secondary organic aerosols formed from different aromatic compounds might contain different chemical composition. However, in the Fig. 3, we can obtain eight same positive laser desorption/ionization mass spectra peaks including m/z 18, 29, 43, 44, 46, 57, 67, 77 from the five aromatic hydrocarbons SOA mass spectra.

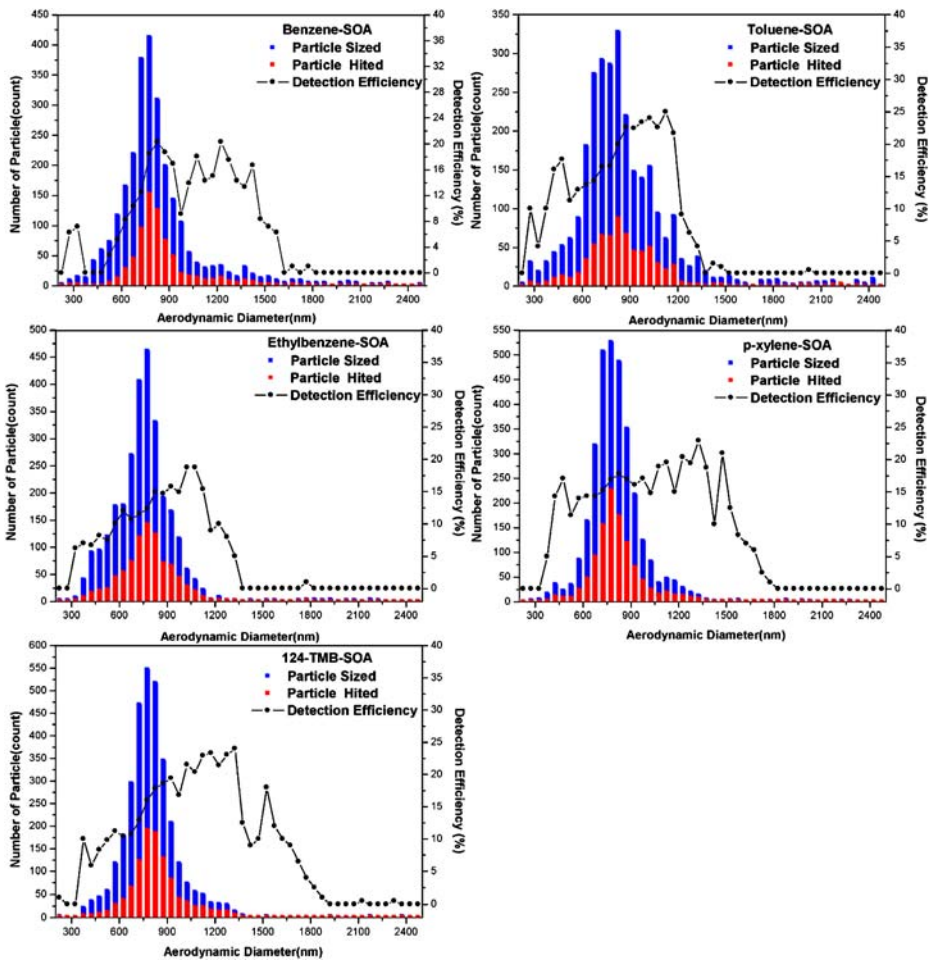
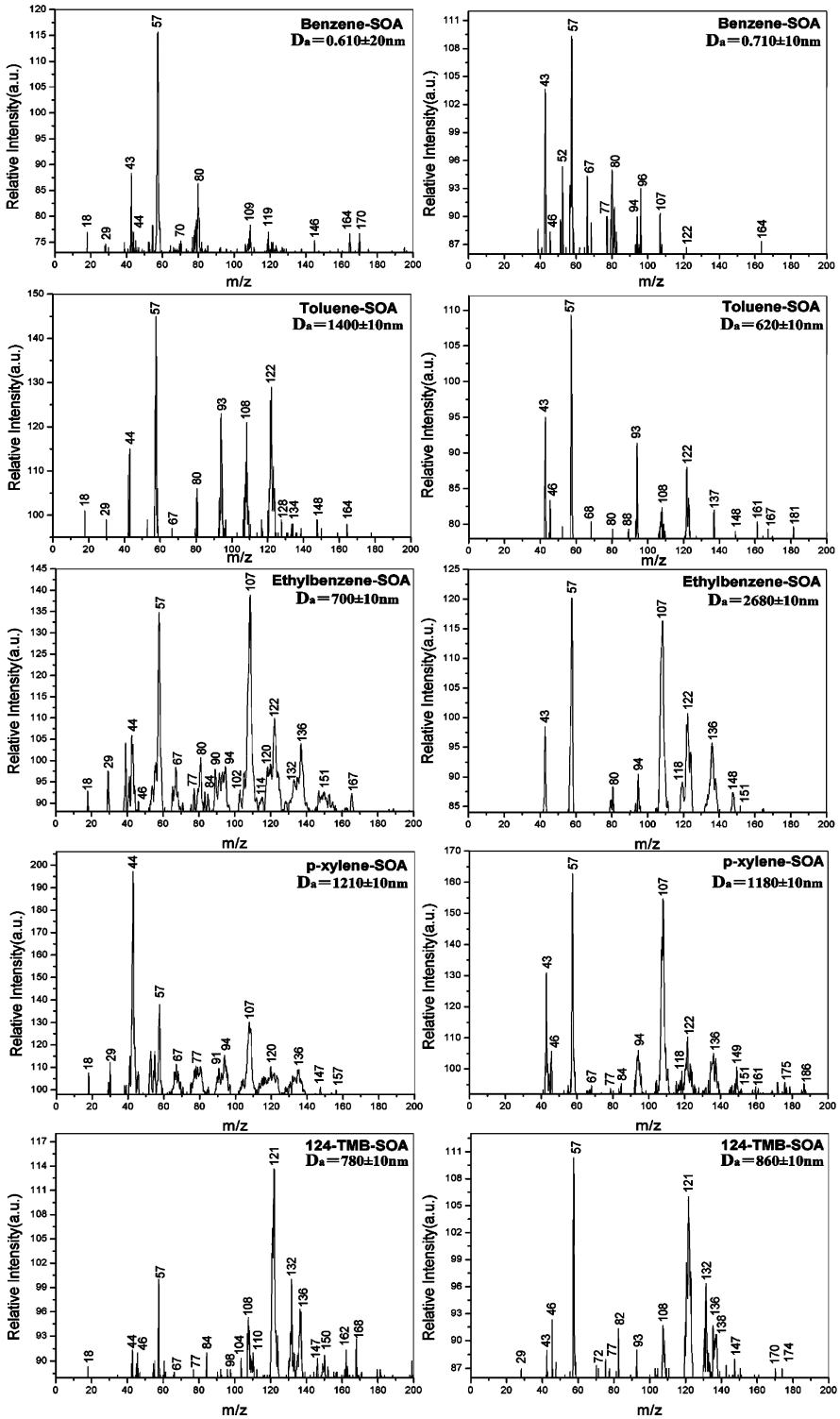


Fig. 2 Detection efficiency and number distribution of five aromatic hydrocarbon SOA particles plotted as a function of particle aerodynamic size

These mass spectra peaks may derive from the fragment ions of the similar products of the photooxidation of aromatic hydrocarbons.

A software was compiled in Visual C++ was developed by our laboratory. Using this software, we can get the total number of mass spectra of the experiment of each aromatic hydrocarbon. Also, the number of mass spectra which contain a certain mass spectra can be obtained. The appearance frequency of the certain mass spectra can be got by the number of mass spectra which contain this certain mass spectra dividing the total number of mass spectra. For example, for the toluene photooxidation experiment, we got total 650 mass spectras, and 329 mass spectras contain m/z 43, so the appearance frequency of m/z 43 is 51%. Appearance frequency of eight mass spectra peaks of five aromatic hydrocarbons SOA are shown in Table 2. From the Table 2, we can see that, the appearance frequency of all eight mass spectra peaks are larger than 8%, the appearance frequency of m/z 43 is larger than 40%, and the appearance frequency of m/z 57 is larger than 70%, these may shown that particles produced



◀**Fig. 3** Aerodynamic size and LDI mass spectra of individual five aromatics SOA particles

from the photooxidation of aromatic hydrocarbons are dominated by the compounds which can be ionized, producing m/z 43 and 57 mass spectra peaks.

3.3 The chemical signatures of the photooxidation products of aromatic hydrocarbons

Mass fragment 44 corresponds to the CO_2^+ fragment and laboratory experiments have shown that it arises, along with a mass fragment 18 (H_2O^+), from decarboxylation of oxo-, and di-carboxylic acid (Alfarra et al. 2004, Alfarra et al. 2006). So the contribution of m/z 18 and 44 indicate that the particles produced from the photooxidation of aromatic hydrocarbons might contain multifunction carboxylic acid species. It is in good agreement with previous reaction chamber studies, where highly oxidized chemical classes from the photooxidation of aromatic compounds including such the oxo-carboxylic acids as glyoxylic acid, 4-oxo-2-pentenoic acid, and 4,5-dioxo-2-pentenoic acid had been reported under different concentration and distribution conditions (Jang et al. 2001).

m/z 29 is signature of the short carbon chain C_2H_5^+ , which is most likely the part of carbon structure of the oxidized compounds discussed above. In addition, HCO^+ fragment arising from carbonyl-containing compounds are likely to contribute to m/z 29 (Alfarra et al. 2006).

Mass fragment 43 arises, typically, from either saturated hydrocarbons of C_3H_7^+ , or from oxidized, carbonyl-containing compound, such as aldehydes and ketones, in the form of CH_3CO^+ (Alfarra et al. 2006), which is more likely to be the case in this study. The formation of aldehyde and ketone compounds has already been reported in a number of chamber studies (Yu et al. 1997, Forstner et al. 1997; Smith et al. 1998; Jang et al. 2001; Edney et al. 2001; Kleindienst et al. 2004). Yu et al. (1997) detected and identified a wide variety of carbonyl products including aromatic aldehydes, di-unsaturated 1,6-dicarbonyls, di-unsaturated 1,4-dicarbonyls resulting from OH-initiated oxidation of aromatic compounds using gas chromatography/mass spectrometric (GC/MS) detection by their O-(2,3,4,5,6-pentafluorobenzyl)-hydroxylamine (PFBHA) derivatives.

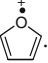
Mass fragment 46 is interpreted as NO_2^+ . Its appearance may imply the formation of nitrogenated organic compounds from each aromatic hydrocarbon, which is also consistent with the reported results. Forstners et al. (1997) studies showed the formation of nitro aromatic and nitrophenolic compounds from the photooxidation of aromatic hydrocarbons

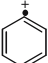
Table 2 Appearance frequency distribution of eight mass spectra peaks of SOAs from five aromatic hydrocarbons

m/z	benzene (%)	toluene (%)	ethylbenzene (%)	<i>p</i> -xylene (%)	1,2,4-TMB (%)
18	18.2±0.5	10.8±0.5	14.6±0.5	56.1±0.5	9.4±0.5
29	8.2±0.5	24.7±0.5	28.1±0.5	17.6±0.5	19.2±0.5
43	42.3±0.5	50.9±0.5	60.2±0.5	68.8±0.5	65.4±0.5
44	23.8±0.5	32.2±0.5	32.6±0.5	33.4±0.5	33.5±0.5
46	22.0±0.5	14.6±0.5	59.3±0.5	39.8±0.5	24.4±0.5
57	91.3±0.5	90.5±0.5	73.2±0.5	89.6±0.5	80.0±0.5
67	19.4±0.5	17.8±0.5	18.3±0.5	23.9±0.5	16.2±0.5
77	18.1±0.5	22.4±0.5	26.6±0.5	22.3±0.5	19.8±0.5

in the presence NO_x . Kleindienst et al (2004) suggested that NO_2 addition to aromatic ring becomes more significant at elevated concentration of NO_2 , which is usually the case in the smog chamber studies. It is explained that the addition of NO_2 can stabilize the ring intermediate leading to the formation of nitro- and di-nitro aromatic compounds.

The mass spectra of the photooxidation products of all five aromatic hydrocarbons are characterized by a very intense mass fragment at m/z 57. It may arise from saturated hydrocarbons of C_4H_9^+ , or from oxidized, dicarbonyl-containing compound, such as di-aldehydes and polyketones, in the form of HCOCO^+ , which is more likely to be the case in this study. The formation of di-aldehyde compounds such as glyoxal and methylglyoxal has already been reported in a number of chamber studies (Yu et al. 1997, Smith et al. 1998; Jang et al. 2001; Edney et al. 2001; Kleindienst et al. 2004). And the recent experiment conducted by Edney et al. (2001) has identified a wide variety of polyketones including 2,3-dioxobutanal, 2-hydroxy-3-oxobutane-1,4-dial, and 2-hydroxy-3,4-dioxopentane-1,5-dial resulting from OH-initiated oxidation of toluene in the presence of NO_x using gas chromatography ion trap mass spectroscopy (GC-ITMS) detection by their O-(2,3,4,5,6-pentafluorobenzyl)-hydroxylamine (PFBHA) derivatives.

m/z 67 fragment may be proposed as . It is shown that the particles produced from the photooxidation of aromatic hydrocarbons may contain furanoid compounds species. Jang et al. (2001) detected and identified furanoid compounds such as furane, methylfuran, 2-furaldehyde, and methyl-2-furadehyde resulting from OH-initiated oxidation of photooxidation of toluene in the presence NO_x .

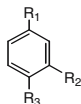
Mass fragment 77 is the signature of . It may come from the particles produced from the photooxidation of aromatic hydrocarbons contained aromatic ring retaining products, which has already been reported in many chamber studies (Yu et al. 1997, Forstner et al. 1997; Smith et al. 1998; Jang et al. 2001; Edney et al. 2001; Kleindienst et al. 2004). These observed aromatic ring retaining products might be the aromatic aldehydes, aromatic acids, nitro aromatic and nitrophenolic.

From our experimental results and discussion mentioned above, it is shown that, the eight same positive laser desorption/ionization MS peaks: $m/z=18, 29, 43, 44, 46, 57, 67,$ and 77 may come from the fragment ions of the products of the aromatic hydrocarbons SOAs: oxo-carboxylic acids, aldehydes and ketones, nitrogenated organic compounds, furanoid and aromatic compounds. Due to the larger appearance frequency of m/z 43 and 57, the contributions of m/z 43 and 57 indicate that the particles produced from the photooxidation of aromatic hydrocarbons are highly oxidized in nature and are dominated by carbonyl-containing compounds.

Some studies have identified SOA products from the photooxidation of aromatics with nitrogen oxides (Yu et al. 1997; Forstner et al. 1997; Smith et al. 1998, 1999; Jang et al. 2001; Edney et al. 2001; Kleindienst et al. 2004). Identified compounds fell into three major classes (1) aromatic ring compounds (e.g., benzaldehyde and 2-methyl-nitrophenol), (2) non-aromatic ring compounds, mainly substituted furans and furanones, including 3-methyl-2,5-furanedione, dihydro-2,5-furanedione, and 2,5-furanedione, (3) ring-opening fragment products, among these products are di-unsaturated 1,6-dicarbonyls, di-unsaturated 1,4-dicarbonyls, saturated dicarbonyls, oxo-carboxylic acids, hydroxy dicarbonyls, glycolaldehyde, hydroxy acetone, and possibly polyketones and epoxy carbonyls. The laser desorption/ionization mass spectra of the organic compounds had been interpreted by Silva and Prather (2002). So it is no surprised that desorption/ionization mass spectra of SOA particles contained m/z 18, 29, 43, 44, 46, 57, 67, 77 mass spectra peaks. Different from

AMS (Alfarra et al. 2006), we can obtain the size and chemical composition of individual SOA particles in real-time, according to a large number of single SOA particles mass spectra, the chemical compositions of SOA were got statistically. As we known, the use of ATOFMS for the analysis of organic compounds in aerosols has been limited because of a lack of knowledge regarding the desorption/ionization and fragmentation processes in the techniques and by the complex mixture of organic species present in atmospheric particles. Our results could provide useful information to distinguish organic aerosol particles from atmospheric particles and infer possible particle emission sources in future field measurement.

3.4 Aromatic hydrocarbons photooxidation mechanism



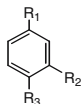
We use  to represent the selected aromatic hydrocarbon (R₁, R₂, R₃=H for benzene; R₁=CH₃, R₂, R₃=H for toluene; R₁=CH₃CH₂, R₂, R₃=H for ethylbenzene; R₁, R₃=CH₃, R₂=H for *p*-xylene; R₁, R₂, R₃=CH₃ for 1,2,4-trimethylbenzene). As shown in Fig. 4, photochemical oxidation of aromatic hydrocarbon is mainly attack by hydroxyl radicals. The OH-initiated aromatic hydrocarbon reaction results in minor H-atom abstraction from the methyl group (for benzene from benzene ring) and major OH addition to the aromatic ring (about 90%) (Atkinson 2000). In the presence of O₂ and NO, the subsequent reactions methylated benzyl radicals lead to the formation of benzaldehyde derivatives. Under atmospheric conditions, the OH-aromatic hydrocarbon adduct formed from the addition pathway reacts with O₂ either by O₂ addition to form (primary) peroxy radicals or by H-abstraction to yield phenolic compounds, or by H-abstraction to form aromatic oxide/oxepin. The fate of the peroxy radicals is governed by competition between reaction with

Fig. 4 Mechanistic diagram for OH-initiated oxidation of aromatic hydrocarbon

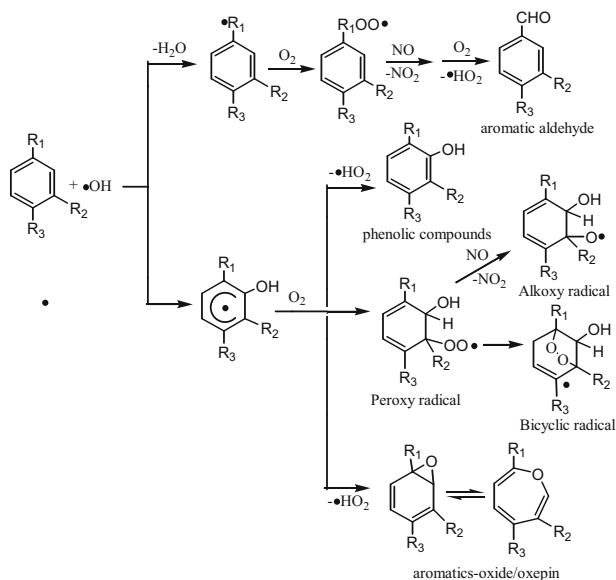
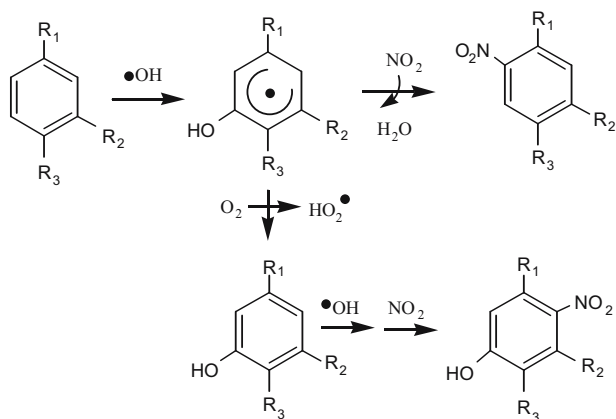


Fig. 5 Proposed reaction mechanisms leading to nitroaromatic and nitrophenols compounds



NO to form alkoxy radicals and cyclization to form bicyclic radicals. Theoretical studies have shown that, instead of reaction with NO, the primary peroxy radicals from OH-initiated oxidation of aromatic hydrocarbon, forming bicyclic radicals. In the presence of NO, subsequent reaction of bicyclic radicals lead to multi-functional organic compound such as glyoxal, methylglyoxal, epoxides, and unsaturated carbonyl compounds (Andino et al. 1996; Atkinson 2000; Suh et al. 2003).

In the presence of NO_2 , as shown in Fig. 5, the OH-aromatic adducts react with NO_2 and produce nitroaromatic (Jang et al. 2001). The phenoxyl radicals can be created through a hydrogen abstraction of phenolic hydrogens by an OH radical and further react with NO_2 , resulting in nitrophenols.

The suggested mechanism for forming furanes from photooxidation of aromatic hydrocarbon is shown in Fig. 6. Furanoid and glyoxal or substituted glyoxal products can be produced through a bridged oxide intermediate on a bicycloring from alkoxy radicals (Jang et al. 2001).

The bicyclic route is a major ring-opening product channel for OH-aromatic hydrocarbon system. Bicyclic radicals resulting from the primary peroxy radicals form secondary peroxy radicals on addition of O_2 which then react with NO to form alkoxy radicals. As presented in Fig. 7, the alkoxy radicals can further decompose to form unsaturated 1,4-dicarbonyls and corresponding α -hydroxy radicals. Subsequent abstraction

Fig. 6 Proposed reaction mechanisms leading to Furanoid compounds

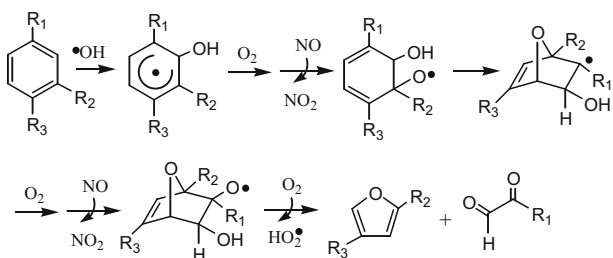
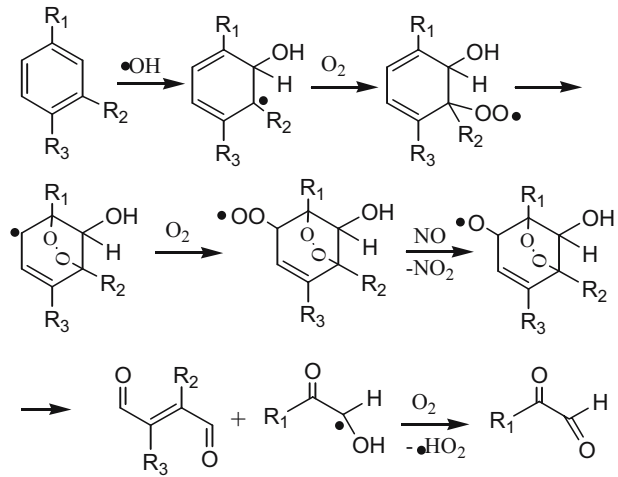


Fig. 7 Proposed reaction mechanisms leading to unsaturated 1,4-dicarbonyls



of α-hydroxyl radicals by O₂ results in the formation of glyoxal or substituted glyoxal (Andino et al. 1996; Jang et al. 2001).

The aromatic-oxide/oxepin is fairly reactive toward OH radicals, with a reaction rate of $2 \times 10^{-10} \text{ cm}^3 \text{ molecule}^{-1} \text{ s}^{-1}$ for toluene-oxide with OH radicals (Klotz et al. 2000). As shown in Fig. 8, addition of OH to C6 position of aromatic-oxide with successive ring cleavage and then H-abstraction by O₂ leads to the formation of unsaturated 1,6-dicarbonyls (Jang et al. 2001).

The atmospheric chemistry of benzene oxide/oxepin has been studied by Klotz et al (1997). Addition of OH to C5 position of aromatic-oxide with successive ring cleavage and then H-abstraction by O₂ leads to the formation of benzoquinones or substituted benzoquinones. Benzoquinones or substituted benzoquinones can be attacked by OH radicals, O₂, and NO, with successive ring cleavage and then H-abstraction by O₂ leads to the formation of dipolyketones or oxo-carboxylic acids product (Jang et al. 2001). These possible reaction pathways are presented in Figs. 9 and 10.

Fig. 8 Proposed reaction mechanisms leading to unsaturated 1,6-dicarbonyls

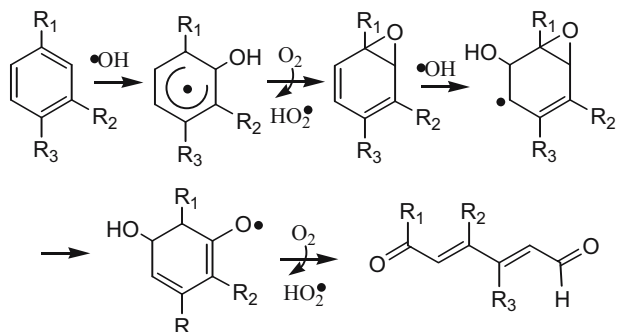
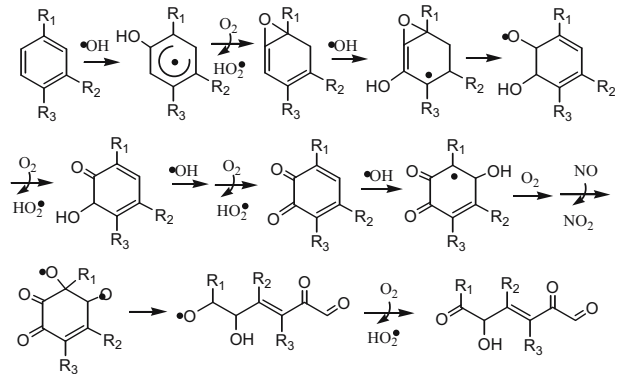


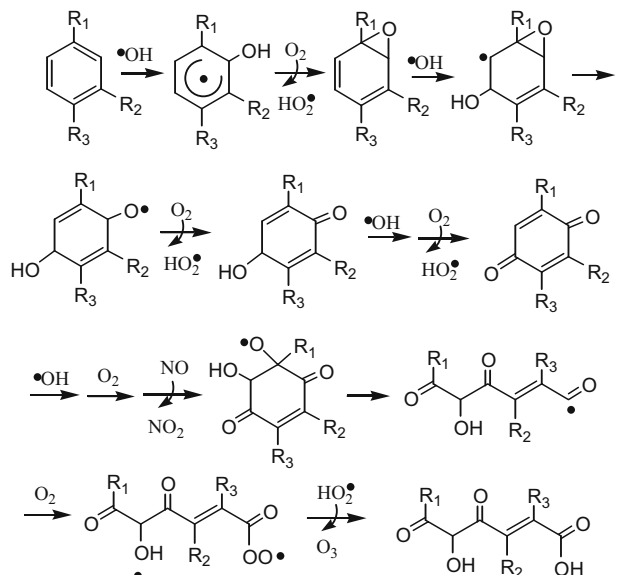
Fig. 9 Proposed reaction mechanisms leading to dipolyketones product



4 Conclusions

A laboratory study was carried out to investigate the secondary organic aerosol products from photooxidation of aromatic hydrocarbons in a smog chamber. The aerosol time of flight mass spectrometer was employed to simultaneously detect the size and composition of the secondary organic aerosol. Different aromatic hydrocarbons SOA mass spectra have 8 same laser desorption/ionization mass spectra peaks: $m/z=18, 29, 43, 44, 46, 57, 67, 77$. These mass spectra peaks may come from the fragment ions of the products of the aromatic hydrocarbons SOA: oxo-carboxylic acids, aldehydes and ketones, nitrogenated organic compounds, furanoid and aromatic compounds. This will provide new information for discussing aromatic hydrocarbon photooxidation reaction mechanism.

Fig. 10 Proposed reaction mechanisms leading to oxo-carboxylic acids product



Acknowledgements This work is supported by National Natural Science Foundation of China (No. 20477043) and Knowledge Innovation Foundation of Chinese Academy of Sciences (KJCX2-SW-H08). The authors express our gratitude to the referees for their value comments.

References

- Alfarra, M.R., Coe, H., Allan, J.D., Bow, K.N., Boudries, H., Canagaratna, M.R., Jimenez, J.L., Jayne, J.T., Garforth, A., Li, S.M., Worsnop, D.R.: Characterization of urban and rural organic particulate in the Lower Fraser Valley using two aerodyne aerosol mass spectrometers. *Atmos. Environ.* **38**, 5745–5758 (2004)
- Alfarra, M.R., Paulsen, D., Gysel, M., Garforth, A.A., Dommen, J., Prévôt, A.S.H., Worsnop, D.R., Baltensperger, U., Coe, H.: A Mass spectrometric study of secondary organic aerosols formed from the photooxidation of anthropogenic and biogenic precursors in a reaction chamber. *Atmos. Chem. Phys.* **6**, 5279–5293 (2006)
- Andino, J.M., Smith, J.N., Flagan, R.C., Goddard, W.A., Seinfeld, J.H.: Mechanism of atmospheric photooxidation of aromatics: a theoretical study. *J. Phys. Chem.* **100**, 10967–10980 (1996)
- Angelino, S., Suess, D.T., Prather, K.A.: Formation of aerosol particles from reactions of secondary and tertiary alkylamines: characterization by aerosol time-of-flight mass spectrometry. *Environ. Sci. Technol.* **35**, 3130–3138 (2001)
- Annamarie, E., Susan, M.L., Jeffrey, R.H., Kevin, J.H., Glen, R.C.: Development of an improved image processing based visibility model. *Environ. Sci. Technol.* **27**, 626–635 (1993)
- Atkinson, R.: Atmospheric chemistry of VOCs and NO_x. *Atmos. Environ.* **34**, 2063–2101 (2000)
- Atkinson, R., Carter, W.P.L., Winer, A.M.: An experimental protocol for the determination of OH radical rate constants with organics using methyl nitrite photolysis as an OH radical source. *J. Air Pollut Control Assoc.* **31**, 1090–1092 (1981)
- Edney, E.O., Driscoll, D.J., Weathers, W.S., Kleindienst, T.E., Conner, T.S., McIver, C.D., Li, W.: Formation of polyketones in irradiated toluene/propylene/NO_x/air Mixtures. *Aero. Sci. Technol.* **35**, 998–1008 (2001)
- Forstner, H.J.L., Flagan, R.C., Seinfeld, J.H.: Secondary organic aerosol from the photooxidation of aromatic: molecular composition. *Environ. Sci. Technol.* **31**, 1345–1358 (1997)
- Gross, D.S., Gälli, M.E., Kalberer, M., Prevot, A.S.H., Dommen, J., Alfarra, M.R., Duplissy, J., Gaeggeler, K., Gascho, A., Metzger, A., Baltensperger, U.: Real-Time measurement of oligomeric species in secondary organic aerosol with the aerosol time-of-flight mass spectrometer. *Anal. Chem.* **78**, 2130–2137 (2006)
- Hao, L.Q., Wang, Z.Y., Huang, M.Q., Pei, S.X., Yang, Y., Zhang, W.J.: The size distribution of the secondary organic aerosol particles from the photooxidation of toluene. *J. Environ. Sci.* **17**, 912–916 (2005)
- Jang, M.S., Kamens, R.M.: Characterization of secondary aerosol from the photooxidation of toluene in the presence of NO_x and 1-propene. *Environ. Sci. Technol.* **35**, 3626–3639 (2001)
- Kleindienst, T.E., Conner, T.S., McIver, C.D., Edney, E.O.: Determination of secondary organic aerosol products from the photooxidation of toluene and their implications in ambient PM_{2.5}. *J. Atmos. Chem.* **47**, 79–100 (2004)
- Klotz, B., Barnes, I., Becker, K.H., Golding, B.T.: Atmospheric chemistry of benzene oxide/oxepin. *J. Chem. Soc. Faraday. Trans.* **93**, 1507–1516 (1997)
- Klotz, B., Barnes, I., Golding, B.T., Becker, K.H.: Atmospheric chemistry of toluene-1,2-oxide/2-methyloxepin. *Phys. Chem. Chem. Phys.* **2**, 227–235 (2000)
- Middlebrook, A.M., Murphy, D.M., Lee, S.H., Thomson, D.S., Prather, K.A., Wenzel, R.J., Liu, D.Y., Phares, D.J., Rhoads, K.P., Wexler, A.S., Johnston, M.V., Jimenez, J.L., Jayne, J.T., Worsnop, D.R., Yourshaw, I., Seinfeld, J.H., Flagan, R.C.: A comparison of particle mass spectrometers during the 1999 Atlanta Supersite Project. *J. Geophys. Res.* **108**, 8424–8436 (2003)
- Odum, J.R., Jungkamp, T.P.W., Griffin, R.J., Flagan, R.C., Seinfeld, J.H.: The atmospheric aerosol-forming potential of whole gasoline vapor. *Science*, **276**, 96–99 (1997)
- Pilinis, C., Pandis, S.N., Seinfeld, J.H.: Sensitivity of direct climate forcing by atmospheric aerosols to aerosol size and composition. *J. Geophys. Res.* **100**, 18739–18754 (1995)
- Prather, K.A., Nordmeyer, T., Salt, K.: Real-time characterization of individual aerosol particles using time-of-flight mass spectrometry. *Anal. Chem.* **66**, 1403–1407 (1994)

- Schwartz, J., Dockery, D.W., Neas, L.M.J.: Is daily mortality associated specifically with fine particles? *Air Waste Manage. Assoc.* **46**, 927–939 (1996)
- Silva, P.J., Prather, K.A.: Interpretation of mass spectra from organic compounds in aerosol time-of-flight mass spectrometry. *Anal. Chem.*, **72**, 3553–3562 (2002)
- Smith, D.F., McIver, C.D., Kleindienst, T.E.: Primary product distribution from the reaction of hydroxyl radicals with toluene at ppb NO_x mixing ratios. *J. Atmos.Chem.* **30**, 209–228 (1998)
- Smith, D.F., McIver, C.D., Kleindienst, T.E.: Primary product distribution from the reaction of OH with *m*-, *p*-xylene, 1,2,4- and 1,3,5-trimethylbenzene. *J. Atmos.Chem.* **34**, 339–364 (1999)
- Suh, I., Zhang, D., Zhang, R.Y., Molina, L.T., Molina, M.J.: Theoretical study of OH addition reaction to toluene. *Chem. Phys. Lett.* **364**, 454–462 (2002)
- Suh, I., Zhang, R.Y., Molina, L.T., Molina, M.J.: Oxidation mechanism of aromatic peroxy and bicyclic radicals from OH-toluene reactions. *J. Am. Chem. Soc.* **125**, 12655–12665 (2003)
- Suess, D.T., Prather, K.A.: Mass spectrometry of aerosols. *Chem. Rev.* **99**, 3007–3035(1999)
- Wang, Z.Y., Hao, L.Q., Zhou, L.Z., Guo, X.Y., Zhao, W.W., Fang, L., Zhang, W.J.: Real-time detection of individual secondary organic aerosol particle from photooxidation of toluene using aerosol time-of-flight mass spectrometer. *Science in China: Series B Chemistry*, **49**, 267–272 (2006)
- Xia, Z.H., Fang, L., Zheng, H.Y., Hu, R., Zhang, Y.Y., Kong, X.H., Gu, X.J., Zhu, Y., Zhang, W.J., Bao, J., Xiong, L.Y.: Real-time measurement of the aerodynamic size of individual aerosol particles. *Acta Physica Sinica.* **53**, 320–324(2004a)
- Xia, Z.H., Fang, L., Zheng, H.Y., Kong, X.H., Zhou, L.Z., Gu, X.J., Zhu, Y., Zhang, W.J.: Real-time measurement of chemical compositions of individual aerosol particles. *Chinese J. Analytical Chemistry*, **32**, 973–976(2004b)
- Yu, J., Jeffries, H.E., Sexton, K.G.: Atmospheric photooxidation of alkylbenzenes–I. Carbonyl product analyses. *Atmos. Environ.* **31**, 2261–2280 (1997)